

Journal Pre-proofs

A study of hydromagnesite and nesquehonite precipitation in indirect aqueous carbonation of thermally-activated serpentine in a batch mode

Sirine Guermech, Julien Mocellin, Lan-Huong Tran, Guy Mercier, Louis-César Pasquier

PII: S0022-0248(22)00028-8
DOI: <https://doi.org/10.1016/j.jcrysgr.2022.126540>
Reference: CRY5 126540

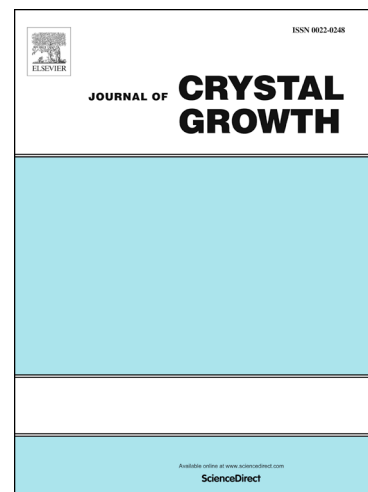
To appear in: *Journal of Crystal Growth*

Received Date: 11 March 2021
Revised Date: 21 December 2021
Accepted Date: 14 January 2022

Please cite this article as: S. Guermech, J. Mocellin, L-H. Tran, G. Mercier, L-C. Pasquier, A study of hydromagnesite and nesquehonite precipitation in indirect aqueous carbonation of thermally-activated serpentine in a batch mode, *Journal of Crystal Growth* (2022), doi: <https://doi.org/10.1016/j.jcrysgr.2022.126540>

This is a PDF file of an article that has undergone enhancements after acceptance, such as the addition of a cover page and metadata, and formatting for readability, but it is not yet the definitive version of record. This version will undergo additional copyediting, typesetting and review before it is published in its final form, but we are providing this version to give early visibility of the article. Please note that, during the production process, errors may be discovered which could affect the content, and all legal disclaimers that apply to the journal pertain.

© 2022 Published by Elsevier B.V.



Journal of Crystal Growth

A study of hydromagnesite and nesquehonite precipitation in indirect aqueous carbonation of thermally-activated serpentine in a batch mode.

Sirine Guermech^a; Julien Mocellin^b; Lan-Huong Tran^c; Guy Mercier^e; Louis-César Pasquier^{d*}

^a Ph.D. Student, Institut national de la recherche scientifique (Centre Eau Terre Environnement), Université du Québec, 490 rue de la Couronne, Québec, Qc, Canada, G1K 9A9, Phone: (418) 654-4677, Fax: (418) 654-2600, email: sirine.guermech@ete.inrs.ca

^b Research Associate, Institut national de la recherche scientifique (Centre Eau Terre Environnement), Université du Québec, 490 rue de la Couronne, Québec, Qc, Canada, G1K 9A9, Phone: (418) 654-2551, Fax: (418) 654-2600, email: julien.mocellin@ete.inrs.ca

^c Research Associate, Institut national de la recherche scientifique (Centre Eau Terre Environnement), Université du Québec, 490 rue de la Couronne, Québec, Qc, Canada, G1K 9A9, Phone: (418) 654-2550, Fax: (418) 654-2600, email: lan.huong.tran@ete.inrs.ca

^d Professor, Institut national de la recherche scientifique (Centre Eau Terre Environnement), Université du Québec, 490 rue de la Couronne, Québec, Qc, Canada, G1K 9A9, Phone: (418) 654-2606, Fax: (418) 654-2606, email: Louis-Cesar.Pasquier@inrs.ca

^e Professor, Institut national de la recherche scientifique (Centre Eau Terre Environnement), Université du Québec, 490 rue de la Couronne, Québec, Qc, Canada, G1K 9A9, Phone: (418) 654-2633, Fax: (418) 654-2600, email: guy.mercier@ete.inrs.ca

*Corresponding author:

Phone: (418) 654-2606, Fax: (418) 654 2600, email: Louis-Cesar.Pasquier@inrs.ca

February 2021

Abbreviations

GHG Greenhouse gases

CCS Carbon Capture and Storage

DIC Dissolved inorganic carbon

Journal Pre-proofs

Abstract

To control and decrease the amount of greenhouse gases in the environment, the process of carbonation is attracting particular attention. Via carbonation, it is possible to control carbon dioxide (CO₂) emissions by using mining residues. This study focuses on the precipitation step of aqueous indirect carbonation of serpentine mining wastes using the actual carbonated solution. To our knowledge, studies of magnesium carbonate precipitation have been based on synthetic solutions only, unlike the process in the present study. Three solutions prepared from the carbonation step with different concentrations were precipitated at temperatures ranging from 25 to 90 °C. The solution contained dissolved magnesium and inorganic carbon in addition to impurities, such as calcium and silica that are initially present in serpentine rock. Nesquehonite precipitated at reaction temperatures of 25, 40 and 50 °C. Hydromagnesite was precipitated at 60, 70, 80, and 90 °C via transition from nesquehonite. The study showed that increasing temperatures accelerate precipitation kinetics and hastens the transition period from nesquehonite to hydromagnesite. The investigation of the effects of the initial supersaturation showed that higher supersaturation promotes a better reaction yield and consequently a better sequestration potential, but lower supersaturation is better for crystal growth. However, supersaturation had no effect on the transition phenomenon from nesquehonite to hydromagnesite. Also, the grain sizes of the resulting minerals had different ranges from those obtained in synthetic solutions. The average size of the nesquehonite in our experiments was around 120 µm, while nesquehonite's size was around 25 µm when prepared from a synthetic solution under relatively comparable operating conditions. The average size of the hydromagnesite was around 50 µm, while its size was around 30 µm when prepared from a synthetic solution, under relatively comparable the same operating conditions.

Keywords: A1. Nucleation, A1. Carbon Sequestration, B1. Magnesium Carbonates, B1.

Nesquehonite, B1. Hydromagnesite, B1. Serpentine.

1. Introduction

Nowadays, greenhouse gases (GHG) have achieved their highest emission rates, and this increase is believed to negatively impact the global climate [1]; hence, efforts to reduce and control these emissions are ongoing. Carbon capture and storage (CCS) is one mitigation procedure among many that aims to reduce anthropogenic carbon dioxide (CO₂) emissions. Mineral carbonation is a CCS technology that safely sequesters carbon in thermodynamically stable carbonate minerals [2]. This process involves the formation of carbonate minerals after reacting liquid or gaseous CO₂ with divalent cations bearing minerals [3].

Carbonation can be achieved using magnesium- and calcium-bearing minerals, such as serpentine, wollastonite, and anorthite [2, 4] from fly ash, steel slag or iron waste [2].

Carbonation can proceed through various methods: (1) direct, (2) indirect, or (3) in a dry or aqueous media. Direct carbonation routes involve just one step for the whole procedure.

Indirect carbonation routes divide the procedure into different steps, such as extraction of the reagents followed by carbonation and then precipitation [2]. With respect to precipitation, the precipitation of magnesium carbonates in the MgO–H₂O–CO₂ system is a complex, multi-stage, and pathway-dependent reaction [5]. A wide range of anhydrous and hydrated magnesium carbonates is formed in nature (Table 1). The most stable mineral form is anhydrous magnesite (MgCO₃) [6, 7]. Despite this fact, magnesite formation at ambient temperature and ambient pressure is impossible for two main reasons: (1) the reaction is kinetically controlled [7-9], (2) the hydrated behaviour of Mg²⁺ [10], and (3) the high dehydration energy of hydrated minerals

[6, 7]. Each Mg^{2+} ion is surrounded by two rings of dipolar water molecules, the first ring contains six molecules while the second contains 12 molecules and is situated at a distance of 4.2 Å from the Mg^{2+} ion [11]. Nesquehonite forms at temperatures below 52 °C [12, 13]. Starting from 52 °C, a transition to another mineral, hydromagnesite occurs [9, 12, 14, 15]. This transition can occur in an aqueous medium [9, 12, 14] either directly from nesquehonite to hydromagnesite [16] or via a transitory mineral dypingite [12, 15, 17]. At higher temperatures, hydromagnesite transforms into magnesite. This transformation process was reported to take between 5 and 15 hours in a $H_2O-CO_2-Na_2CO_3-MgCl_2$ solution at 120 °C and a partial pressure of $P_{CO_2} = 3$ bar [7]. Another study reported magnesite formation between 80 and 120 °C and a pressure of 1 and 2.5 bar in an $NaCl-MgCl_2-NaHCO_3-HCl-NaOH$ system [18]. Magnesite was also synthesized at 90 °C for 15 hours and also at 60 °C for seven days after ethylenediaminetetraacetic acid (EDTA) addition in an attempt to produce magnesite at moderate temperatures [19].

Table 1: Possible formed mineral in the $MgO-H_2O-CO_2$ system

Brucite	$Mg(OH)_2$
Artinite	$(Mg_2CO_3)(OH)_2 \cdot 3H_2O$
Lansfordite	$MgCO_3 \cdot 5H_2O$
Nesquehonite	$MgCO_3 \cdot 3H_2O$
Dypingite	$(Mg_5)(CO_3)_4(OH)_2 \cdot 6H_2O$
Hydromagnésite	$(Mg_5)(CO_3)_4(OH)_2 \cdot 5H_2O$
Magnésite	$MgCO_3$

Studying the supersaturation of a chemical reaction and its impact on the products are of paramount importance since supersaturation controls the precipitation process, determines the amount of growth and the agglomeration phenomena, and influences the grain size distribution [20-22]. A study focusing on the effects of supersaturation of nesquehonite at 40 °C showed that higher supersaturation leads to smaller grain size and to higher agglomeration occurrence [13].

Other studies investigating supersaturation of nesquehonite from 15 °C to 60 °C [23] and hydromagnesite at 80 °C [24] showed that the higher the supersaturation rates are, the lower the grain size distribution of the minerals becomes. It is also reported that higher nesquehonite supersaturation leads to a shorter induction time [25].

Supersaturation is linked to crystal growth rates [26]. For hydromagnesite, the study of hydromagnesite supersaturation from 25 to 75 °C led to the conclusion that growth occurs via adsorption to the growth units [26]. It was also reported that growth rates are enhanced by higher hydromagnesite supersaturation [24]. When comparing various studies concerning supersaturation of magnesium carbonates in an MgO–H₂O–CO₂ solution, it was found that supersaturation values did not correlate with growth rates [5]; hence, it was concluded that the precipitation of magnesium carbonates are heavily dependent on the process and on the reaction pathway [5]. This fact highlights the complexity of the reaction. Thus, magnesium carbonate precipitation depends on the process thus, investigating our own system was a key element to revealing its particularities.

This paper focuses on the precipitation step of the indirect aqueous carbonation process founded and studied by our research team [27-33]. The process aims to safely store anthropogenic CO₂ along with exploiting mining wastes of the magnesium-rich serpentine mineral, which is a variation of the serpentine rock. The latter presents a large feedstock in southern Quebec and is a great asset for carbon sequestration [34]. The indirect carbonation process in this study consisted of extracting magnesium from a preheated serpentine pulp and concurrently dissolving CO₂ in it followed by precipitation of the resulting solution.

The thermal treatment that serpentine mineral undergoes promotes better magnesium leaching via destruction of the hydroxyl that initially hinders the dissolution phenomenon [35]. A

weighed amount of metaserpentine was mixed with tap water. The resulting pulp undergoes a gas flux of CO_2 in which magnesium is leached, and inorganic carbon is concurrently dissolved. Thus, a solution rich in magnesium and dissolved inorganic carbon (DIC) along with impurities, such as silica and calcium, was obtained at a selected temperature and duration. Later, magnesium carbonates were precipitated from this solution.

Many studies have focused on the precipitation of magnesium carbonates for CO_2 mitigation insights or fundamental studies using a synthetic solution [14, 18, 26, 36-38] gathering the main reaction component from various sources (such as K_2CO_3 , $\text{Mg}(\text{NO}_3)_2$, MgCl_2 , Na_2CO_3 , and others). In this study, the precipitation process of magnesium carbonate in an $\text{MgO-H}_2\text{O-CO}_2$ system and the transition from nesquehonite to hydromagnesite were investigated. The particularly unique nature of this work is that all studied solutions are real, non-synthetic (unlike the ones mentioned above), and dedicated for carbonation purposes only. This process, once investigated, will be used in the future on an industrial scale for CO_2 mitigation. Studies available in the literature have focused on the precipitation of magnesium carbonates based on synthetic solutions. Synthetic solutions do not fully mimic the production of carbonates on an industrial scale within a CSS process. Moreover, they contain important amounts of impurities that are not normally found in a real solution (such as Cl in a solution with MgCl_2). Reagents are also heated separately to the reaction temperature and skipping the heating phase is unavoidable in the industrial process. Thus, those differences would affect ionic strength, crystallization process, growth, grain size and quality of the resulting minerals.

Overall, the aim of this study was investigate several parameters: (1) understand nucleation and growth kinetics of nesquehonite and hydromagnesite; (2) study the transition from nesquehonite to hydromagnesite; (3) assess the effects of temperature and supersaturation on the precipitation and the transition from nesquehonite to hydromagnesite and consequently,

the sequestration potential of the procedure; and (4) identify the physicochemical characteristics (composition, grain size distribution, purity, and mineral phase) of the minerals generated under various conditions from a solution prepared via a mineral carbonation procedure.

2. Materials and methods

2.1. Raw material preparation

Mining wastes consisting of serpentine were collected from the old chromite site near Thetford Mines of southern Quebec (Canada). The samples represented all heterogeneity in composition and size. The material was crushed by a jaw crusher and ground by a ball mill. The residues were then activated by heat treatment at 650 °C for 30 min using a rotary kiln and finally ground with an IsaMill until the median size is $D_{50} = 10 \mu\text{m}$. The chemical composition of the samples was 42% MgO, 41% SiO₂, 8.2 % Fe₂O₃, 0.9 % Al₂O₃, 0.01% CaO, and 11.6% was lost upon ignition. The latter analysis was performed by inductively-coupled plasma spectrometry of emission (ICP-AES, Varian Vista AX CCD Simultaneous ICP-AES, Palo-Alto, CA, USA) after fusion by lithium metaborate (Corporation Scientifique Claisse, Quebec, Canada).

2.2. Carbonation experiments

The aqueous mineral carbonation of serpentine mining residues was carried out in a 4L Parr reactor, model 4550 (Parr Instrument Company®, Moline, Illinois). Carbonation proceeded via a reaction containing 1%, 3%, and 5% serpentine pulp densities fed to 100% CO₂ feed gas at ambient temperature ($20 \pm 5 \text{ }^\circ\text{C}$) and pressure of 80 PSI. The stirring speed was set to 600 rpms. Each carbonation reaction lasted 30 min. Temperatures, pressures, and stirring speeds were controlled using a *ParrCom* recorder. The solution was filtered through vacuum filtration on a Whatman 934- AH glass microfiber filter (pore size = 1.5 μm). A quantity of 10 mL of the solution

acidified with 1 mL of concentrated HNO_3 was kept as the mother solution for ICP-AES analysis. Hence, three solutions with different initial concentrations were obtained (L1–3). Initial concentrations of Mg^{2+} were about 1,000, 2,500, and 5,000 mg/L, respectively.

2.3. Precipitation experiments

Precipitation experiments were performed with 500 mL of each carbonation solution (L1–3). The runs were performed in a 500 mL jacketed glass vessel connected to a temperature controller thermostat (CF15, Julabo, Germany). The suspension was stirred at 300 rpm with two 45° angled blades made of polytetraethylfluoroethylene (PTFE). The stirring was performed with a mechanical stirrer. Each solution was tested under different temperatures (25, 40, 50, 60, 70, 80 and 90°C). Each experiment lasted 6 h without considering the heating time from room temperature to reaction temperature. pH and conductivity were measured by a XL600 Accumet Fisher Scientific multimeter equipped with a double-junction ColeParmer electrode with an Ag/AgCl reference cell. Measurements were continuously recorded during the entire experiment via Accumet Comm software. Liquid and solid samples were collected during the experiment for further chemical analysis. At the end of each experiment, the solution was filtered using a microfiber Whatman 934-AH filter of 1.5 μm pore size. The precipitated crystals were washed with pure water and then dried at 50 °C for 10 h. The carbonates were also analyzed using ICP-AES after fusion by lithium metaborate. Dissolved inorganic carbon (DIC) was analyzed by infrared spectroscopy TOC-VCPH, Shimadzu. Grain size distribution was analyzed by a laser type particle size analyzer, HORRIBA-LA950. The structure and morphology of the final products and their evolution over the course of the experiments were examined by scanning electron microscopy (SEM; Zeiss EVO® 50 smart SEM).

3. Theory and calculation

3.1. Calculation of precipitation yield

The precipitation yield of each reaction is defined as the amount of the converted dissolved magnesium to solid carbonates and is calculated as shown below:

$$\text{Precipitation yield (\%)} = \frac{m_t - m_f}{m_t} \times 100 \quad (1)$$

in which m_t and m_f are the masses of the total dissolved magnesium before and after precipitation, respectively.

3.2. Activity coefficient model

The activity coefficient model is based on the value of the ionic strength (I). The latter is calculated according to the following equation:

$$I = \frac{1}{2} \sum_i C_i Z_i^2 \quad (2)$$

in which Z_i is the charge of an ion, i , and C_i is the concentration of the ion i in mol/L. The ionic strength of the solution was varied between 0.5 and 1.5. The activity coefficient model chosen for this work was based on a study by Truesdell and Jones (Truesdell & Jones, 1974). As the latter model is based on molality, all the necessary unit conversions were considered. The model was embedded in PHREEQC V3 software [39]. The database was the WATEQ4F. The latter was associated with the selected model.

3.3. Solubility constant and supersaturation

The solid–liquid equilibrium reactions of nesquehonite and hydromagnesite are outlined as shown below.

For nesquehonite:



For hydromagnesite:



From equations (3) and (4), it is possible to calculate the supersaturation of each mineral, which is the ratio of activity products divided by the solubility product (K_{sp}).

The K_{sp} of each mineral was obtained as described below:

For nesquehonite (see equation 3):

$$K_{sp-nesq} = (a_{eqMg^{2+}}) \cdot (a_{eqCO_3^{2-}}) \cdot (a_{eqH_2O})^3 \quad (5)$$

a_{eq} is the activity coefficient of the correspondent element at equilibrium (see equation 2).

For hydromagnesite (see equation 4):

$$K_{sp-hydrm} = (a_{eqMg^{2+}})^5 \cdot (a_{eqCO_3^{2-}})^4 \cdot (a_{eqOH^-})^2 \cdot (a_{eqH_2O})^4 \quad (6)$$

Supersaturation for nesquehonite was obtained as described below:

$$S_{nesq} = \frac{a_{Mg^{2+}} \cdot a_{CO_3^{2-}} \cdot a_{H_2O}^3}{K_{sp-nesq}} \quad (7)$$

a is the activity coefficient of each reactant of the solution.

For the hydromagnesite, supersaturation was obtained as shown below:

$$S_{hydrom} = \frac{a_{Mg^{2+}}^5 \cdot a_{CO_3^{2-}}^4 \cdot a_{OH^-}^2 \cdot a_{H_2O}^4}{K_{sp-hydrm}} \quad (8)$$

Chemical speciation and supersaturation were calculated using PHREEQC V3. The database was modified to include $K_{sp-hydrm}$ under various temperatures as described by Gautier et al. [26].

4. Results and discussion

4.1. Characterization of solutions L1, L2, and L3

L1–3 are solutions prepared via carbonation using densities of 1%, 3%, and 5% serpentine pulp, respectively. They are mainly characterized by the presence of impurities represented as wt% of 9.7, 7.4 and 4.4 for L1–3, respectively, out of the total ion percentages. These impurities are generally absent in synthetic solutions. The main impurities present in the solution are silica and calcium. They constitute, on average, 3.1 wt.% and 1.2 wt.%, respectively, of the total ions in the solution. The rest of impurities are, on average, listed in order: (1) 0.8 wt.% sulfur, (2) 0.5 wt.% sodium, (3) 0.4 wt.% potassium, (4) 0.16 wt.% chrome, (5) 0.1 wt.% iron, (6) 0.1 wt.% nickel, and (7) 0.1 wt. zinc. The impurities depend mainly on carbonation parameters, namely, serpentine pulp density, gas pressure, and carbonation step duration. Table 2 shows the concentration of elements in each mother liquor.

Table 2: Concentration in mg/L of Mg and other components in the initial solution L1, L2, and L3

	Mg	Ca	Cr	Fe	K	Na	Ni	S	Si	Zn	DIC*
L1	1025	41.1	3.52	0.14	22.9	29.60	3.35	26.3	79.1	0.06	930
L2	2083	48.41	5.67	0.50	25.4	30.23	4.89	39.6	144	0.50	1863
L3	5019	54.51	16.9	1.00	30.6	30.50	5.51	66.2	236	2.98	4453

4.2. Effect of supersaturation and temperature on the reaction yield

The precipitation yield of each solution at each temperature is presented in Table 3. It is shown that for solutions L1–3, the yield of Mg precipitation increases with temperature. For L1, the percentage of precipitation reaches 2.3% at 25 °C and 89% at 90 °C. Solutions L2 and L3 show the same pattern of reaction yield. Thus, it can be concluded that the reaction yield and kinetics increase with temperature increase as observed by many authors [7, 22, 38]. Now, for each reaction temperature, it is noted that increasing the initial concentration leads to an increase in

the reaction yield. For L1 at 25 °C, the reaction yield was low (2.3%) from the initial value of 1010 to 976.7 mg/L at the end of the experiment. With an increase in the initial concentration (L3), this value dramatically increases to 42% from 4962 to 2877.9 mg/L.

Table 3 : Effect of temperature on precipitation yield of Mg after 6 h.

Temperature (°C)	25	40	50	60	70	80	90
Reaction yield for L1 (%)	2.3	25.7	38	55	70.21	79.03	89
Reaction yield for L2 (%)	8.4	37.6	36.7	56.7	78.3	86.1	94.1
Reaction yield for L3 (%)	42	62.4	71.3	78.1	94.4	96.3	97.7

4.3. Effect of temperature on the mineral phase and morphology of the final product

For the series with three experiments in each series, SEM image analyses showed a typical nesquehonite needle-like morphology precipitated from 25 to 50°C regardless of supersaturation level (Fig. 1. a.b.c). These observations are in agreement with many authors who studied the morphology of magnesium carbonates at low temperatures ranging from 10 to 50 °C even though some of them used a synthetic solution [9, 12, 13, 15, 25, 40].

At 60 °C regardless of the supersaturation level, the crystals still showed a needle-like shape, in which they were covered with tiny sphere-like sheets. The latter observation suggests that the nesquehonite to hydromagnesite transition is still occurring. Davies and Bubela [12] confirmed

that the nesquehonite–hydromagnesite transition starts at 52 °C and continues as temperature increases.

At 70, 80, and 90 °C, the crystals exhibited a sphere-like, platy morphology of hydromagnesite (Fig. 1. e,f,g,h). Many authors have also reported findings of the same morphology at such temperature [7, 9, 12, 15, 22, 26, 40].

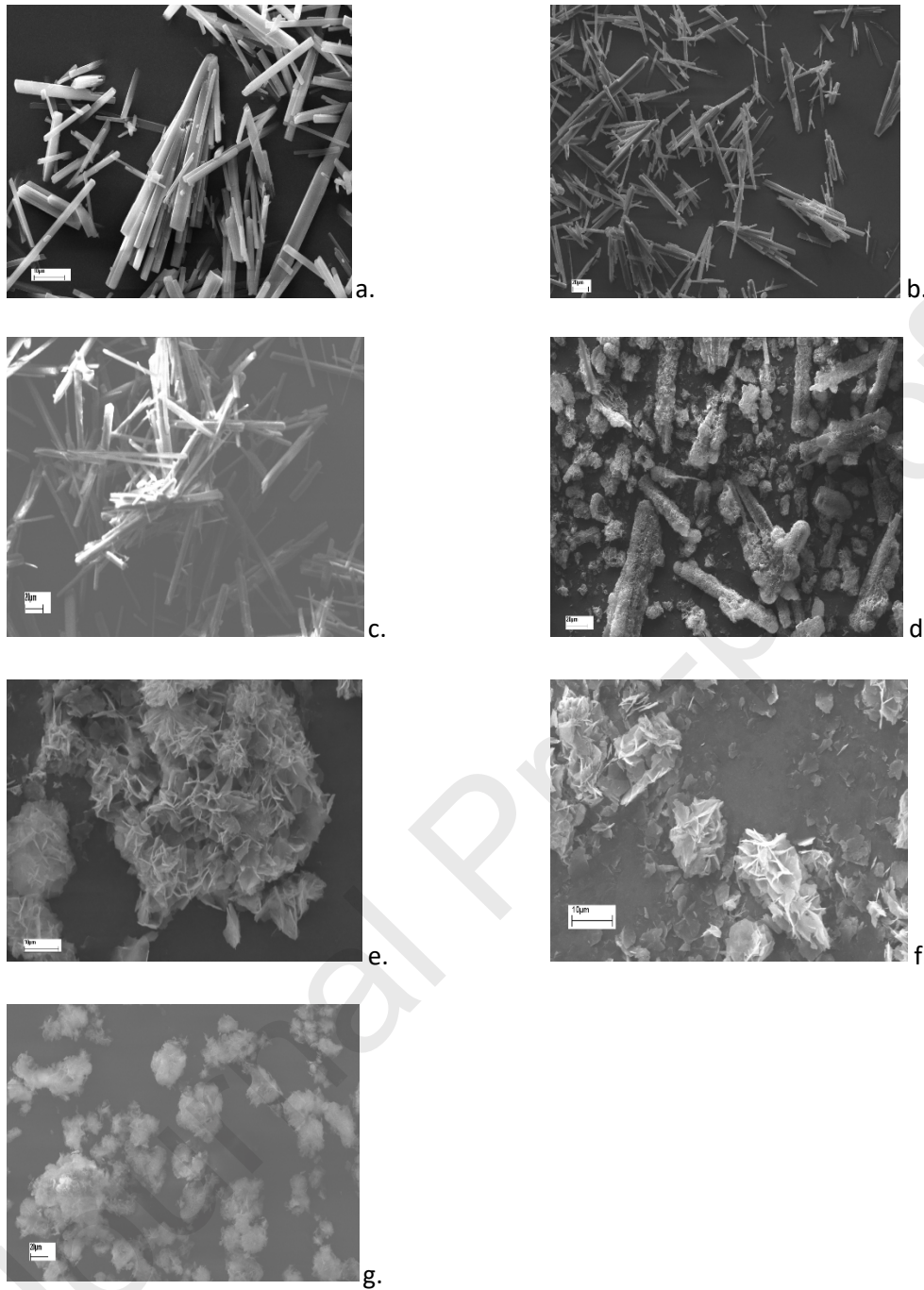


Figure 1: Morphology of the final products according to temperature (a) 25°C; (b) 40°C; (c) 50°C; (d) 60°C; (e) 70°C; (f) 80°C; (g) 90°C

4.4. Study of supersaturation

The initial solutions were supersaturated with respect to nesquehonite at room temperature:

(1) For L1, $S_{\text{nesq}} = 0.2 \pm 0.05$, (2) for L2, $S_{\text{nesq}} = 1.5 \pm 0.05$, and (3) for L3, $S_{\text{nesq}} = 2.5 \pm 0.05$. As for

supersaturation with respect to hydromagnesite at room temperature, its values are given: (1) For L1, $S_{\text{hydrom}} = 56 \pm 5$ for L2, (2) $S_{\text{hydrom}} = 117 \pm 5$, and (3) for L3, $S_{\text{hydrom}} = 250 \pm 6$. Supersaturation with respect to both nesquehonite and hydromagnesite were plotted versus reaction time, which included the heating period (Fig. 2.). Although the solutions were heavily supersaturated with respect to hydromagnesite and marginally supersaturated with respect to nesquehonite, nesquehonite was the first mineral phase that formed. The more rapidly formed mineral (nesquehonite) was favored over the more stable one (hydromagnesite) [9]. This order indicates that kinetics in this reaction were favored over thermodynamics [7]. This phenomenon was confirmed by SEM images. At 25, 40, and 50 °C, nesquehonite (Fig. 1. a, b, and c) was the present mineral phase. At 60 °C and higher, hydromagnesite was the dominant mineral phase (Fig. 1. d to g).

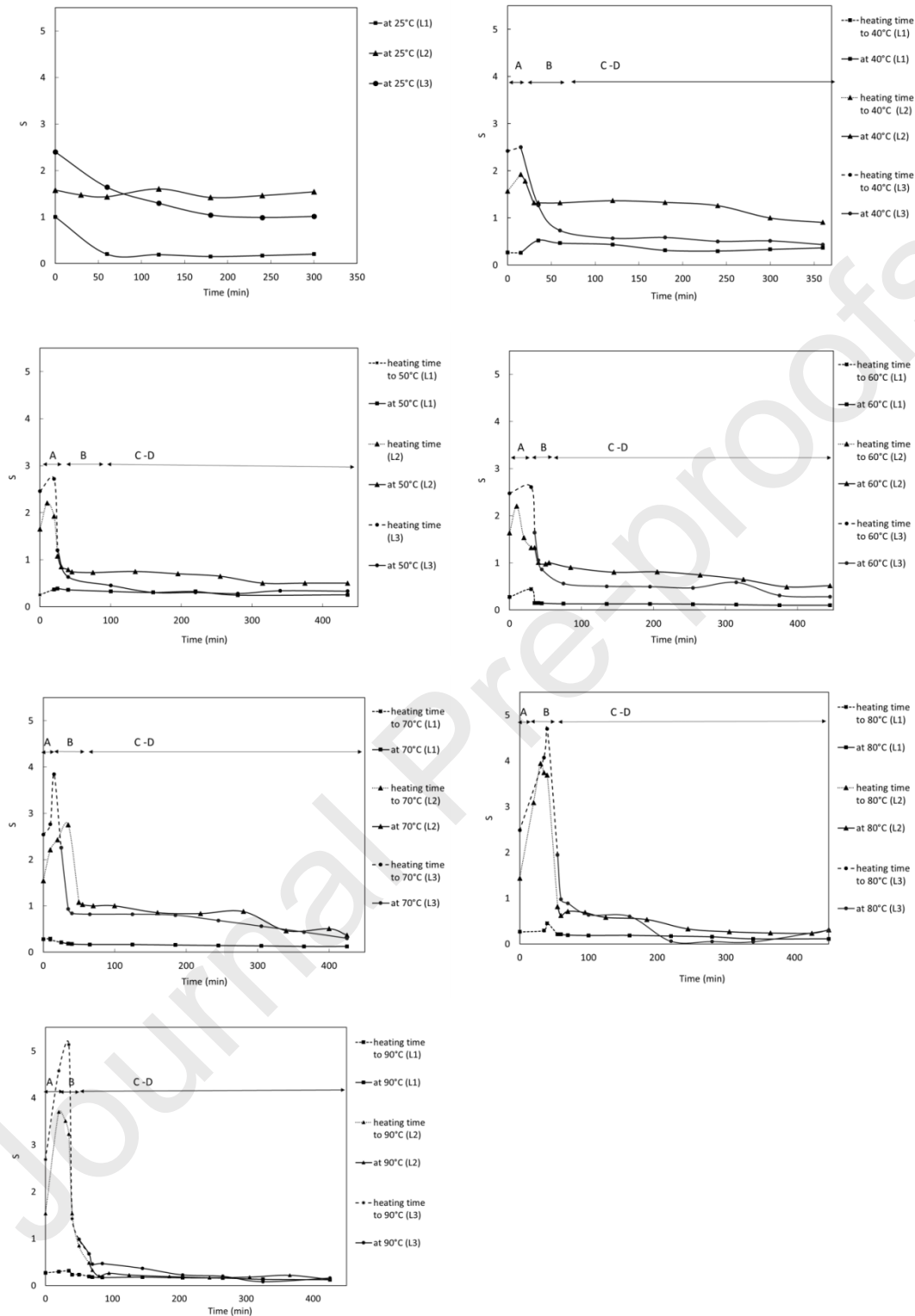


Figure 2: Supersaturation of nesquehonite versus reaction time at different temperatures. A is the nucleation phase. Phase B represent the growth phase coupled to nucleation. Growth continues in phases C and D after which ripening starts. Phase D represent the rip

The curves present in Figs. 2 and 3 correspond to the supersaturation of nesquehonite and hydromagnesite, respectively (obtained by equations 8 and 9, respectively). These curves exhibited similar evolution patterns during the course of time, which were shown as increase in supersaturation during the heating phase (phase A), reaching a peak, dropping sharply (phase B), and then slowly decreasing until reaching a plateau (phase C to D) [41].

Examining the curves of Fig. 2., it can be noted that from 25 to 60 °C, the values of supersaturation increased due to heating until they reached a peak (phase A). It was noted during the experiments that nucleation had already been occurring before reaching the peak, suggesting that the activation energy barrier of nesquehonite had been overcome. The latter was estimated to be 69.8 KJ.mol⁻¹ in a MgCl₂-NaCO₃ system by Cheng and Li [25]. Phase A corresponds to the beginning of the nucleation phenomenon. Small nuclei started to form until reaching a critical size, a process that forms a stable embryo that will trigger growth after overcoming the activation energy barrier.

For each experiment starting from the same initial concentration, the peak's value of supersaturation increases with increasing reaction temperature. For L2, the peak's value is 1.9 at a reaction temperature of 40 °C. The peak in the same solution at 50 °C shows a value of 2.4. This finding indicates the important effect of temperature on the supersaturation value.

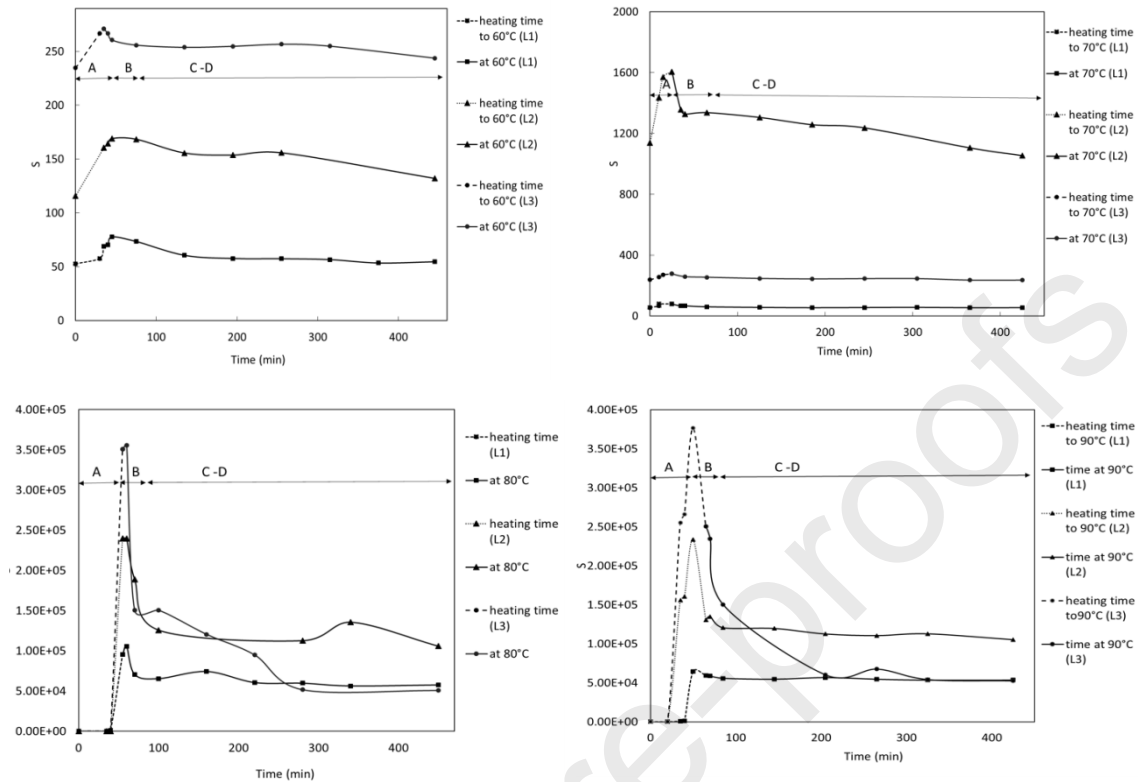


Figure 3: Supersaturation of hydromagnesite versus reaction time at different temperatures. A is the nucleation phase. Phase B represent the growth phase coupled to nucleation. Phase C and D are phases in which growth continues, and ripening starts. Phase D represent the r

The sharp drop in S_{nesq} over a short time span indicates the ongoing phenomenon of nucleation along with a more emphasized growth phenomenon (phase B). A plateau was reached in each experiment, a finding that suggests the ripening phase according to Ostwald rule (phase C to D) [42].

Examining the curves of Fig. 3., it can be noted that the curves exhibit the same patterns as those for nesquehonite (Fig. 2). Supersaturation did not correlate with hydromagnesite formation in any aspect. It is noted that for all experiments regardless of the supersaturation value, hydromagnesite appeared at the same time for each reaction temperature thus overcoming of the barrier of the activation energy. The latter was estimated to be 45.5 ± 9 KJ.mol^{-1} after examining hydromagnesite precipitation in a synthetic solution of $\text{MgCl}_2 \cdot 6\text{H}_2\text{O}$

and Na_2CO_3 [26]. At 60 and 70 °C, hydromagnesite appeared in phases C and D on curves of both nesquehonite and hydromagnesite. At 80 °C, hydromagnesite appeared shortly after phase B had started. At 90 °C, hydromagnesite appeared in phase A. It should be noted that at high reaction temperatures of 80 and 90 °C, the ones with the fastest kinetics, S_{hydrom} curves of L3 and L1 converged at some point in time. They attained close values of supersaturation $S_{\text{hydrom}} = 5.10^4$, regardless of the initial concentration. Thus, starting from different supersaturation levels at the same temperature and ending with close supersaturation values suggest that the reaction is temperature-dependent.

4.5. Effect of temperature and supersaturation on the grain size distribution

Table 4 displays the average particle size D_{50} and the particles' span ($D_{90}-D_{10}/D_{50}$) in each experiment. Overall and from 25 to 90°, no specific tendency of the grain size distribution was found. For the nesquehonite mineral from 25 to 50°, D_{50} tended to decrease from 140 µm for L2 and L3 to 40.65 and 20.39 µm, respectively. In contrast, the span increased for L2 from 2.63 at 25 to 5.42 at 50 °C and for L3 from 1.85 at 25 to 2.12 at 50 °C. This increase suggests a widening of the size distribution range. Cheng and Li [13] noted an increase in the average particle size from 17.18 µm at 25 °C to 32.91 µm at 40°C and a parallel decrease in the span from 1.63 at 25 °C to 1.17 at 40 °C. The nesquehonite crystals were obtained at supersaturation levels ranging from 6 to 12 over a 4 h reaction time in an MgCl_2 - NaCO_3 system and a stirring speed of 300 rpm with no heating period. The increase in size and decrease in the span were attributed to the fact that a higher temperature causes an increase in the collision rate. An increase in the collision rate will induce more nuclei forming and elevate the probability of coalescence, a process that favors growth.

Table 4: D_{50} and span of the grain size distribution

Temperature	25	40	50	60	70	80	90
D_{50} (μm)							
L1	-	145.34	120.32 \pm	29.34	51.45	68.32	67.32
		\pm 5.20	4.43	\pm 3.41	\pm 5.2	\pm 2.21	\pm 1.34
L2	140.81	102.62	105.05 \pm	40.65	40.75	62.51	69.49
	\pm 4.05	\pm 3.54	3.87	\pm 4.21	\pm 4.32	\pm 0.67	\pm 0.32
L3	140.54	136.89	112.55 \pm	20.39 \pm	26.07 \pm	28.23 \pm	24.85
	\pm 6.05	\pm 5.86	2.76	4.45	2.36	0.24	\pm 0.55
Span (D_{90}-D_{10}/D_{50})							
L1	-	4.21	6.32	2.71	1.88	1.92	1.76
		\pm 0.05	\pm 0.03	\pm 0.01	\pm 0.02	\pm 0.07	\pm 0.03
L2	2.63	4.86	5.42	2.93	1.78	1.86	1.64
	\pm 0.32	\pm 0.05	\pm 0.56	\pm 0.02	\pm 0.01	\pm 0.02	\pm 0.31
L3	1.85	1.64	2.12	3.65	1.41	1.48	1.84
	\pm 0.23	\pm 0.2	\pm 0.3	\pm 0.02	\pm 0.01	\pm 0.03	\pm 0.05

For hydromagnesite particles, D_{50} increased from 29.34 to 67.32 μm for L1 over the temperature range of 60 to 90 $^{\circ}\text{C}$, from 40.65 to 69.49 μm for L2, and from 20.39 to 24.85 μm for L3. Also, it is noticeable that the span became narrower as the temperature increased. Cheng and Li (2010) [22] obtained hydromagnesite via a MgCl_2 - NaCO_3 with a maximum supersaturation of $1.52 \cdot 10^9$, an average reaction of 2 h, and a stirring speed of 300 rpm. The authors noted a parallel

increase in D_{50} from 30.92 μm at 60 °C to 45.66 μm at 90 °C as the reaction temperature increased.

The span decreased from 3.25 at 50 °C to 0.06 at 90 °C.

Wang and Li (2012) [43] noted an increase in the average size of both nesquehonite and hydromagnesite with temperature increases and claimed that higher temperature are more suitable for crystal growth. The particles were obtained in a range of temperature between 30 and 90 °C in an $\text{MgCl}_2\text{-CO}_2\text{-NH}_3\text{-H}_2\text{O}$ system of a continuous mixed-suspension–mixed-removal crystallizer at a stirring speed of 300 rpm. The value of D_{50} evolved from 8 to 30 μm at 50 and 90 °C.

From Table 4, it can be seen that hydromagnesite particles are smaller at higher supersaturation. In this case, lower supersaturation favors crystal growth, while higher supersaturation favors primary nucleation. This observation is consistent with Myerson, Erdemir and Lee [44] and Wang and Li [43]. A study noted that at 300 rpm, the crystals' length at 40 and 50 °C was 64.64 and 80.2 μm , respectively [45].

The results of grain distribution of the present study exhibit differences from those studies found in the literature [13, 22, 43, 45]. On average, D_{50} of this present paper is about 125 μm for nesquehonite and 44 μm for hydromagnesite. These values resulted from the fact that the solution used in this study was non-synthetic and prepared from the carbonation procedure of serpentine and CO_2 . Since the solution was not synthetic, the reactants were not separable as in the case of a $\text{MgCl}_2\text{-CO}_2\text{-NH}_3\text{-H}_2\text{O}$ or a $\text{MgCl}_2\text{-NaCO}_3$ system and would undergo heating before reaching the reaction temperature. Separating components followed by heating them separately was not preferred because real precipitation on an industrial scale will heat the solution from room temperature.

Investigating temperature effects on the particle sizes of nesquehonite and hydromagnesite is a paramount step when scaling up the technology to an industrial scale, especially when it comes to the filtration process and valorization of the products. Particle size has a direct impact on the filtration process, and many papers have been dedicated to study this phenomenon [46-48]. From these facts, the need to study the precipitation phase from a solution prepared from a carbonation process dedicated for carbon sequestration has emerged. Also, the grain size highlights the rapid growth kinetics, which is encouraging for the CCS process.

4.6. Nesquehonite to hydromagnesite transition

The mineral transition was followed by collecting solid samples during precipitation reactions at 50 °C and higher and examining them via SEM. Transition was found to occur at 60 °C and higher. Even if the precipitation at 50 °C lasted 6 h, no hydromagnesite was present (Fig 1**Error! Reference source not found.**c). Table 5 sums up different data at temperatures of 60, 70, 80, and 90 °C related to the transition. It was attempted to related different parameters to the transition phenomenon. When the transition occurred, neither S_{nesq} nor S_{hydrom} were steady or showed a particular tendency toward transition. However, what attracts attention is the time at which the transition occurs and its corresponding temperature. The transition for 60, 70, and 80 °C occurred at 240, 120, and 12 min, respectively, after reaching the reaction temperature regardless of the supersaturation levels of the parent solution and regardless of the actual value of S_{nesq} and S_{hydrom} at the transition time. At 90 °C, the transition occurred during the heating phase when the temperature reached 84 °C. The transition took 49 min to complete starting at 25 °C for all different solutions. This observation indicates that the transition is a time- and temperature-dependent phenomenon. Davies and Bubela [12] also reported that the transition from nesquehonite to hydromagnesite depends on time and temperature. Also, it could be noted from these results (Table 5) that the higher the temperature is, the faster the transition

period. This finding indicates that higher temperatures accelerate the transition process, which is in agreement with Hänchen, Prigiobbe, Baciocchi and Mazzotti [7].

Table 5: Supersaturation, time, and temperature of the nesquehonite to hydromagnesite transition.

	60 °C			70 °C			80 °C			90 °C		
	L1	L2	L3	L1	L2	L3	L1	L2	L3	L1	L2	L3
S_{nesq} transition	0.1	0.59	0.21	0.15	0.61	0.8	0.18	0.58	0.63	0.21	0.8	0.4
S_{hydrom} transition	53	132	255	56	124	246	65	126	150	60	160	300
Time after first transition spotted (minutes)	240	240	240	120	120	120	12	12	12	49	49	49
Temperature at first transition (°C)	60	60	60	70	70	70	80	80	80	84	84	84
Duration after which transition is fully completed (minutes)	>240	>240	>240	165	165	165	30	30	30	10	10	10

The transition indicates that the activation energy of hydromagnesite could be estimated at 45.5 ± 9 KJ.mol⁻¹ [26]. This transition was reported to occur directly from nesquehonite to hydromagnesite [16] in addition to transitory dypingite minerals [9, 12, 15, 17].

The transition of nesquehonite to hydromagnesite is complete after 240, 165, and 30 min at 60, 70, and 80 °C, respectively. At 90 °C, the transition began at 84 °C, and was complete after 10 min at approximately 89.4 °C. From this finding, it is noted that the higher the temperature is, the shorter the transition duration.

4.7. Purity of the final products

Regarding the fact that impurities are present in the precipitation solution, carbonates were analyzed. The purity of samples has reached 99% in average for both nesquehonite and hydromagnesite. Calcium and silica together represent 1% of the carbonate composition with 0.3% calcium and 0.7% silica. This finding suggests that the average of 7% of impurities, present initially in the precipitation solution, has no impact on the product quality regardless of the supersaturation level and temperature. This finding also confirms that the transition from nesquehonite to hydromagnesite was not affected by the presence of impurities. A study by Cheng and Li (2010) [22] reported a high purity of MgO after the calcination of hydromagnesite at 800 °C. The mineral was produced in an $\text{MgCl}_2\text{-Na}_2\text{CO}_3$ medium, which is considered highly impure compared to the study used in the present study [22].

4.8. Scale up from laboratory to industrial scale

To assess the relevance of this work on an industrial scale, it is necessary to highlight the differences between laboratory and industrial scale. Many parameters, such as the schedule of the solution heating, will surely be different on this scale. For this process, a total of six experiments were conducted. Six solutions with the same initial supersaturation, $[\text{Mg}^{2+}] = 3100$ mg/L, were heated from room temperature to 40 and 80 °C on a different heating schedule. The details of the heating schedule along with mean grain size D_{50} are provided in Table 6.

Table 6: Parameters of heating schedule and the associated grain size results.

Heating schedule			
40 °C	0.25 °C per min	0.5 °C per min	1 °C per min
D_{50} (μm)	50.3	91.8	125.2
80 °C	0.25 °C per min	0.5 °C per min	1 °C per min
D_{50} (μm)	25.2	41.4	71.2

Figure 4 and Figure 5 show the evolution of the concentration of the solution starting from the same initial solution but undergoing a different heating schedule to respectively 40 and 80 °C. At each temperature during heating, the concentration of magnesium is perfectly comparable to the same temperature of another experiment with a different heating schedule. It is also noted that at the end of each experiment, the concentration of each solution is the same at each temperature even if the heating rate is different. From this, it can be concluded that the heating schedule has little, even no effect, on the concentration during the precipitation process as this process depends entirely on the precipitation temperature. Nevertheless, it is noted that the heating schedule impacts the grain size. According to Table 6, for nesquehonite, at 40 °C the grain size increased from 50.3 to 125.2 μm when the heating schedule increased respectively from 0.25 °C per minute to 1 °C per minute. For hydromagnesite at 80 °C, the grain size increased from 25.2 to 71.2 μm when the heating schedule increased from 0.25 to 1 °C per min. So, when scaling up the process, it is expected that shortening the heating time will contribute to reducing the grain size while increasing the heating schedule will lead to an increase in grain size.

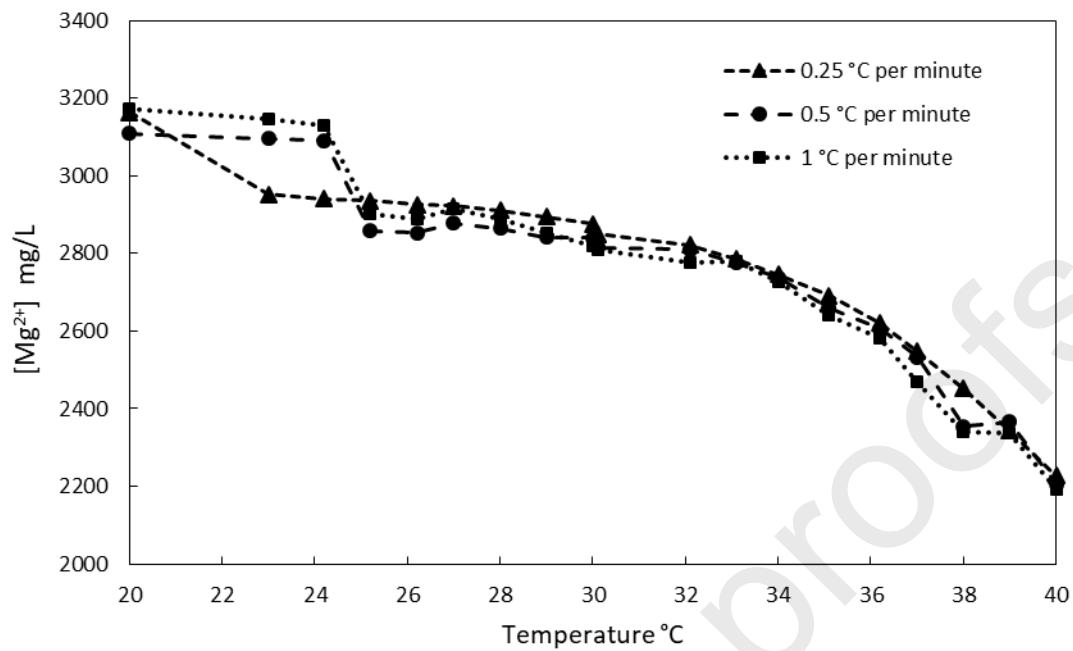


Figure 4: Evolution of the concentration of dissolved magnesium according to different heating schedule from room temperature to 40 °C.

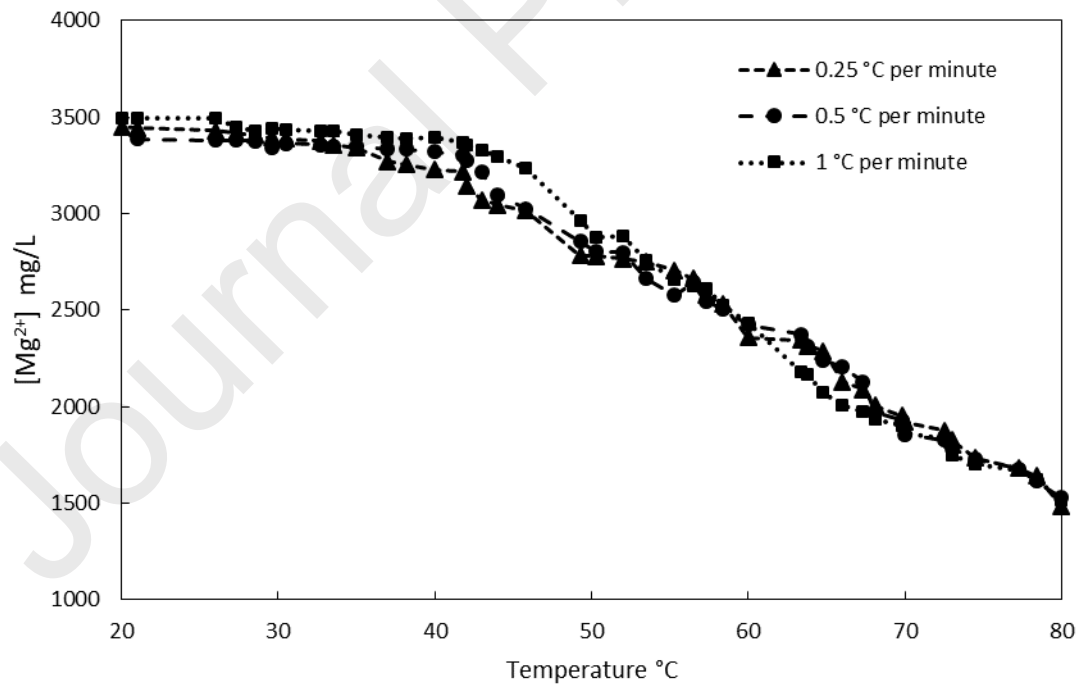


Figure 5: Evolution of the concentration of dissolved magnesium according to different heating schedule from room temperature to 80 °C.

4.9. CO₂ sequestration potential

This study emphasizes the sequestration potential of serpentine residue (a variation of the serpentine mineral) by indirect aqueous means via producing magnesium carbonate in batch mode. Magnesium was leached from a preheated serpentine by reacting it in a CO₂ gas stream under certain pressure. Hence, a solution loaded with Mg and DIC was obtained. The concentration of Mg²⁺ and DIC depends on the carbonation procedure itself and its different aspects, such as the heat treatment of serpentine, its particle size, CO₂ gas stream pressure, the amount of serpentine used, and the reaction duration [27, 28, 31-33].

Once the solution was filtered, it was ready for precipitation. The precipitation phase plays a direct role in determining the amount of the gross sequestered CO₂ percentage. From this determination, the importance of studying the precipitation phase of magnesium carbonates in a non-synthetic, dedicated for carbon sequestration solution arose.

The gross CO₂ sequestration potential could be improved by increasing the reaction yield, which in turn led to an increase in the presence of a higher reaction temperature and higher supersaturation level. Supersaturation was controlled during the carbonation phase.

Temperature and duration of the reaction affects sequestration potential. Optimizing these two parameters causes a reduction in energy consumption.

On an industrial scale, it is important to discern the transition time, temperature, and duration as these factors will also affect the sequestration potential. Nesquehonite has a sequestration with 31.81% CO₂. Hydromagnesite contains 37.64% CO₂. Balancing energy consumption (by studying precipitation phase) and the amount of sequestered carbon will certainly lead to optimum energy consumption and sequestration potential.

The environmental implications of this procedure can be summarized as described below:

- (1) Safe and permanent storage of CO₂ emitted from the industrial sector.
- (2) The use and valorization of mining wastes, such as magnesium-rich ultramafic rocks.
- (3) Formation of highly pure carbonates that could be useful for further purposes

5. General discussion

Currently, most studies concerning the precipitation of magnesium carbonates use synthetic solutions to study the growth phenomena and kinetics of carbonate precipitation. The operating conditions during the tests carried out with synthetic solutions are generally far from an industrial application. For example, when testing with synthetic solutions, the solutions are heated separately to the desired temperature before coming into contact, and the solutions also contain impurities, such as Cl, that are not present in real solutions.

The present paper's results were compared to those in literature. Several differences in chemical composition between synthetic and real solution exist: (1) the absence of some impurities (Fe, Si, Ca, K, Cr, Ni, Z, S) and (2) the presence of other impurities with high concentrations when compared with the concentrations of Mg and Cl⁻, thus causing an effects on ionic strength and consequently the formation of minerals and the transition process (such as when MgCl₂ is the source of magnesium, $[Mg^{2+}] = 2[Cl^-]$). Also, salts, such as MgCl₂, also affect the formation of hydrated species by reducing the water layer surrounding Mg²⁺ ions and by impacting the behavior of water molecules by reducing water chemical activity [6].

The main differences between literature and the present study were found to be the grain size of both nesquehonite and hydromagnesite. The D₅₀ value of nesquehonite ranged from 102 to 145 μm under different supersaturation levels, different temperatures, and at 300 rpm. The median size of nesquehonite reported in the literature was found to be remarkably smaller than

the median size of the present paper (from 4.56 to 32.91 μm under relatively comparable supersaturation and stirring speed from 200 to 400 rpm) [13, 23].

The D_{50} of hydromagnesite ranged from 62 to 68 μm , for L1 and L2, at 80 ° and 90 °C and at 300 rpm. For L3, the D_{50} value of hydromagnesite was 26 μm on average at 80 ° and 90 °C and at 300 rpm. In the literature, the median size of hydromagnesite ranged from 8 to 45.66 μm at temperatures ranging from 50 to 90 °C when carbonates were synthesized in $\text{MgCl}_2\text{-Na}_2\text{CO}_3$ and $\text{MgCl}_2\text{-CO}_2\text{-NH}_3\text{-H}_2\text{O}$ systems [22, 43]. The median size of hydromagnesite in a $\text{MgSO}_4\text{-(NH}_4\text{)CO}_3$ was found to be 64 μm at 40 °C and 80.2 μm at 50 °C .

Another benefit of using real solutions in this study is the transition period. For each temperature, the time needed for the nesquehonite-to-hydromagnesite transition at 60, 70, 80 and 90°C under close conditions to those on the pilot and industrial scales could be determined. Regardless of the similarities and differences between the results presented in literature and in the present paper and regardless of how much data are available about magnesium carbonates precipitation, mimicking the industrial process on a laboratory scale via a real solution is always challenging. It represents the characteristics of solutions used in a CSS procedure. Hence the result of studying such solutions yields the fundamental characteristics and right insight into what will be obtained when upscaling on pilot and industrial levels.

This study is of paramount importance to carbon capture and utilisation (CCU) as understanding the precipitation reaction of magnesium carbonates enables control of their properties.

Magnesium carbonates have extensive applications, such as pharmaceutical use, construction material synthesis, cement industry, and even cosmetics.

This study enables the basic understanding of the precipitation aspects of magnesium carbonate precipitation from thermally-activated serpentine and dissolved CO_2 . It is the first step toward a

population balance analysis and a kinetic study (nucleation, growth, and agglomeration rates) that is key step to designing an effective industrial process for satisfactory CSS and CCU.

6. Conclusion

The mother solutions were prepared from a carbonation procedure of serpentine mining residues and a gas flow of 100% CO₂. Three sets of tests were run, each with a different initial concentration. The supersaturation was calculated based on the Truesdell and Jones model. The effects of supersaturation combined with effects of temperature were investigated on the final product and on the transition phenomenon from nesquehonite to hydromagnesite. Several conclusions were drawn:

- a) Increasing temperatures have an accelerating effect on the reaction yield. Higher supersaturation levels also have an accelerating effect. The more the solution is supersaturated, the more the precipitation yield increases.
- b) Temperature and supersaturation affect mineralogy. From 25 °C to 50 °C, nesquehonite is formed. From 50 °C to 90 °C, hydromagnesite is formed.
- c) Grain size distribution also depends on supersaturation and temperature. Increasing temperature causes a decrease in grain size. Increasing supersaturation also causes a decrease in grain size.
- d) Grain size distribution of nesquehonite and hydromagnesite were found to be remarkably higher than those made in synthetic solutions that have been reported in literature.
- e) The transition from nesquehonite to hydromagnesite and its duration depends strongly on time and temperature. For a single temperature, a certain timeframe and no matter what supersaturation, the transition point is always the same.

- f) Precipitation of magnesium carbonates from a carbonation solution containing 10% impurities had no effect on the mineralogy or on the purity of the product impurities and did not interfere with the precipitation phase.
- g) Grain size distribution is remarkably higher than those values reported in the literature using synthetic solution.

Acknowledgements

This work was supported by NSERC Research and Development Collaboration grant RDCPJ 522524-17.

References

- [1] GIEC, Changements climatiques 2014: Rapport de synthèse. Contribution des Groupes de travail I, II et III au cinquième Rapport d'évaluation du Groupe d'experts intergouvernemental sur l'évolution du climat, GIEC, Genève, Suisse, 2014, pp. 161.
- [2] W.J.J. Huijgen, R.N.J. Comans, Carbon dioxide sequestration by mineral carbonation. Literature Review, Energy research Centre of the Netherlands ECN, 2003.
- [3] W. Seifritz, CO₂ disposal by means of silicates, *Nature*, 345 (1990) 486.
- [4] K.S. Lackner, D.P. Butt, C.H. Wendt, Progress on binding CO₂ in mineral substrates, *Energy Conversion and Management*, 38 (1997) S259-S264.
- [5] E. Swanson, K. Fricker, M. Sun, A.-H. Park, Directed precipitation of hydrated and anhydrous magnesium carbonates for carbon storage, *Physical chemistry chemical physics : PCCP*, 16 (2014).
- [6] C.L. Christ, P.B. Hostetler, Studies in the system MgO-SiO₂-CO₂-H₂O (II); the activity-product constant of magnesite, *American Journal of Science*, 268 (1970) 439-453.
- [7] M. Hänchen, V. Prigiobbe, R. Baciocchi, M. Mazzotti, Precipitation in the Mg-carbonate system—effects of temperature and CO₂ pressure, *Chemical Engineering Science*, 63 (2008) 1012-1028.
- [8] E. Koenigsberger, L.-C. Königsberger, H. Gamsjager, Low-temperature thermodynamic model for the system Na₂CO₃ – MgCO₃ – CaCO₃ – H₂O, 1999.
- [9] L. Hopkinson, P. Kristova, K. Rutt, G. Cressey, Phase transitions in the system MgO–CO₂–H₂O during CO₂ degassing of Mg-bearing solutions, *Geochimica et Cosmochimica Acta*, 76 (2012) 1-13.
- [10] F.L. Sayles, W.S. Fyfe, The crystallization of magnesite from aqueous solution, *Geochimica et Cosmochimica Acta*, 37 (1973) 87-99.
- [11] W. Bol, G.J.A. Gerrits, C.L. van Panthaleon Eck, The hydration of divalent cations in aqueous solution. An X-ray investigation with isomorphous replacement, *Journal of Applied Crystallography*, 3 (1970) 486-492.
- [12] P.J. Davies, B. Bubela, The transformation of nesquehonite into hydromagnesite, *Chemical Geology*, 12 (1973) 289-300.
- [13] W. Cheng, Z. Li, Precipitation of nesquehonite from homogeneous supersaturated solutions, *Crystal Research and Technology*, 44 (2009) 937-947.
- [14] Z. Zhang, Y. Zheng, Y. Ni, Z. Liu, J. Chen, X. Liang, Temperature- and pH-Dependent Morphology and FT-IR Analysis of Magnesium Carbonate Hydrates, *The Journal of Physical Chemistry B*, 110 (2006) 12969-12973.
- [15] L. Hopkinson, Ken Rutt, G. Cressey, The Transformation of Nesquehonite to Hydromagnesite in the System CaO-MgO-H₂O-CO₂: An Experimental Spectroscopic Study, *The Journal of Geology*, 116 (2008) 387-400.
- [16] Z. Hao, F. Du, Synthesis of basic magnesium carbonate microrods with a “house of cards” surface structure using rod-like particle template, *Journal of Physics and Chemistry of Solids*, 70 (2009) 401-404.
- [17] D. Langmuir, Stability of Carbonates in the System MgO-CO₂-H₂O, *The Journal of Geology*, 73 (1965) 730-754.
- [18] G.D. Saldi, G. Jordan, J. Schott, E.H. Oelkers, Magnesite growth rates as a function of temperature and saturation state, *Geochimica et Cosmochimica Acta*, 73 (2009) 5646-5657.
- [19] G. Montes-Hernandez, M. Bah, F. Renard, Mechanism of formation of engineered magnesite: A useful mineral to mitigate CO₂ industrial emissions, *Journal of CO₂ Utilization*, 35 (2020) 272-276.

- [20] J.W. Mullin, *Crystallization*, Butterworth Heinemann, Oxford, UK., 2001.
- [21] H. Hojjati, M. Sheikhzadeh, S. Rohani, Control of Supersaturation in a Semibatch Antisolvent Crystallization Process Using a Fuzzy Logic Controller, *Industrial & Engineering Chemistry Research*, 46 (2007) 1232-1240.
- [22] W. Cheng, Z. Li, Controlled Supersaturation Precipitation of Hydromagnesite for the $\text{MgCl}_2\text{-Na}_2\text{CO}_3$ System at Elevated Temperatures: Chemical Modeling and Experiment, *Industrial & Engineering Chemistry Research*, 49 (2010) 1964-1974.
- [23] Y. Wang, Z. Li, G.P. Demopoulos, Controlled precipitation of nesquehonite ($\text{MgCO}_3\cdot 3\text{H}_2\text{O}$) by the reaction of MgCl_2 with $(\text{NH}_4)_2\text{CO}_3$, *Journal of Crystal Growth*, 310 (2008) 1220-1227.
- [24] J. Wang, Z. Li, Crystallization and Agglomeration Kinetics of Hydromagnesite in the Reactive System $\text{MgCl}_2\text{-Na}_2\text{CO}_3\text{-NaOH-H}_2\text{O}$, *Industrial & Engineering Chemistry Research*, 51 (2012) 7874-7883.
- [25] W. Cheng, Z. Li, Nucleation kinetics of nesquehonite ($\text{MgCO}_3\cdot 3\text{H}_2\text{O}$) in the $\text{MgCl}_2\text{-Na}_2\text{CO}_3$ system, *Journal of Crystal Growth*, 312 (2010) 1563-1571.
- [26] Q. Gautier, P. Bénézech, V. Mavromatis, J. Schott, Hydromagnesite solubility product and growth kinetics in aqueous solution from 25 to 75°C, *Geochimica et Cosmochimica Acta*, 138 (2014) 1-20.
- [27] L.-C. Pasquier, Procédé de piégeage du CO_2 industriel par carbonatation minérale de résidus miniers silicatés (serpentine) et valorisation des sous-produits., Institut national de la recherche scientifique, Université du Québec, Institut national de la recherche scientifique, Québec, 2014, pp. 250.
- [28] L.-C. Pasquier, G. Mercier, J.-F. Blais, E. Cecchi, S. Kentish, Parameters optimization for direct flue gas CO_2 capture and sequestration by aqueous mineral carbonation using activated serpentine based mining residue, *Applied Geochemistry*, 50 (2014) 66-73.
- [29] L.-C. Pasquier, G. Mercier, J.-F. Blais, E. Cecchi, S. Kentish, Reaction Mechanism for the Aqueous-Phase Mineral Carbonation of Heat-Activated Serpentine at Low Temperatures and Pressures in Flue Gas Conditions, *Environmental Science & Technology*, 48 (2014) 5163-5170.
- [30] L.-C. Pasquier, G. Mercier, J.-F. Blais, E. Cecchi, S. Kentish, Technical & economic evaluation of a mineral carbonation process using southern Québec mining wastes for CO_2 sequestration of raw flue gas with by-product recovery, *International Journal of Greenhouse Gas Control*, 50 (2016) 147-157.
- [31] C. Du Breuil, L. César-Pasquier, G. Dipple, J.-F. Blais, M.C. Iliuta, G. Mercier, Mineralogical Transformations of Heated Serpentine and Their Impact on Dissolution during Aqueous-Phase Mineral Carbonation Reaction in Flue Gas Conditions, *Minerals*, 9 (2019) 680.
- [32] C. Du Breuil, L.C. Pasquier, G. Dipple, J.-F. Blais, M.C. Iliuta, G. Mercier, Impact of particle size in serpentine thermal treatment: Implications for serpentine dissolution in aqueous-phase using CO_2 in flue gas conditions, *Applied Clay Science*, 182 (2019) 105286.
- [33] I. Tebbiche, L.-C. Pasquier, G. Mercier, J.-F. Blais, S. Kentish, Thermally activated serpentine leaching under flue gas conditions in a bubble column reactor operated at ambient pressure and temperature, *Hydrometallurgy*, 195 (2020) 105391.
- [34] F. Huot, G. Beaudoin, R. Hébert, M. Constantin, G. Dipple, M. Raudsepp, Le piégeage du CO_2 anthropique dans les parcs à résidus d'amiante du sud du Québec: Concept et valorisation, Université Laval, Géologie et génie Géologique, Faculté des sciences et de génie, Québec, Canada, 167 (2003).
- [35] M.J. McKelvy, R. Sharma, A.V.G. Chizmeshya, R.W. Carpenter, K. Streib, Magnesium Hydroxide Dehydroxylation: In Situ Nanoscale Observations of Lamellar Nucleation and Growth, *Chemistry of Materials*, 13 (2001) 921-926.

- [36] A.L. Harrison, V. Mavromatis, E.H. Oelkers, P. Bénézech, Solubility of the hydrated Mg-carbonates nesquehonite and dypingite from 5 to 35 °C: Implications for CO₂ storage and the relative stability of Mg-carbonates, *Chemical Geology*, 504 (2019) 123-135.
- [37] S. Hariharan, M. Mazzotti, Growth Kinetics of Synthetic Hydromagnesite at 90 °C, *Crystal Growth & Design*, 17 (2017) 317-327.
- [38] M.J.M. Correia, Optimisation de la précipitation des carbonates de magnésium pour l'application dans un procédé de la séquestration du CO₂ par carbonatation minérale de la serpentine. , Institut Nationale de la Recherche Scientifique, 2017, pp. 105.
- [39] D.L. Parkhurst, C. Appelo, Description of input and examples for PHREEQC version 3: a computer program for speciation, batch-reaction, one-dimensional transport, and inverse geochemical calculations, US Geological Survey, 2013.
- [40] W. Cheng, Z. Li, G.P. Demopoulos, Effects of Temperature on the Preparation of Magnesium Carbonate Hydrates by Reaction of MgCl₂ with Na₂CO₃, *Chinese Journal of Chemical Engineering*, 17 (2009) 661-666.
- [41] P. François, V. Stéphane, M. Denis, Cristallisation Aspects théoriques, Techniques de l'ingénieur Opérations unitaires : extractions fluide/fluide et fluide/solide, base documentaire : TIB332DUO (2005).
- [42] T. Threlfall, Structural and Thermodynamic Explanations of Ostwald's Rule, *Organic Process Research & Development*, 7 (2003) 1017-1027.
- [43] D. Wang, Z. Li, Gas-Liquid Reactive Crystallization Kinetics of Hydromagnesite in the MgCl₂-CO₂-NH₃-H₂O System: Its Potential in CO₂ Sequestration, *Industrial & Engineering Chemistry Research*, 51 (2012) 16299-16310.
- [44] A.S. Myerson, D. Erdemir, A.Y. Lee, *Handbook of Industrial Crystallization*, Cambridge University Press, Cambridge, 2019.
- [45] X. Geng, L. Lv, C. Li, T. Zhang, B. Liang, Y. Chen, S. Tang, The kinetics of CO₂ indirect mineralization of MgSO₄ to produce MgCO₃·3H₂O, *Journal of CO₂ Utilization*, 33 (2019) 64-71.
- [46] R. Wakeman, The influence of particle properties on filtration, *Separation and Purification Technology*, 58 (2007) 234-241.
- [47] S. Tarleton, R. Wakeman, *Solid/liquid separation: equipment selection and process design*, Elsevier 2006.
- [48] G. Moody, P. Norman, *Chemical pre-treatment, Solid-Liquid Separation: Scale-up of industrial equipment*. Oxford: Elsevier, (2005) 38-81.

Figure captions

- Figure 1** Morphology of the final products according to temperature
(a)25°C; (b) 40°C; (c) 50°C; (d) 60°C; (e) 70°C; (f) 80°C; (g) 90°C
- Figure 2** Supersaturation of nesquehonite versus reaction time at different temperatures. A is the nucleation phase. Phase B represent the growth phase coupled to nucleation. Growth continues and ripening starts during phases C and D. Phase D represent crystal ripening.
- Figure 3** Supersaturation of nesquehonite versus reaction time at different temperatures. A is the nucleation phase. Phase B represent the growth phase coupled to nucleation. Growth continues and ripening starts during phases C and D. Phase D represents crystal ripening.
- Figure 4** Evolution of the concentration of dissolved magnesium according to different heating schedule from room temperature to 40 °C.
- Figure 5** Evolution of the concentration of dissolved magnesium according to different heating schedule from room temperature to 80 °C.

Tables

Table 1	Possibly formed mineral in the MgO–H₂O–CO₂ system
Table 2	Concentration in mg/L of Mg and other components in the initial solution L1, L2, and L3
Table 3	Effect of temperature on precipitation yield after 6 h
Table 4	D₅₀ and span of the grain size distribution
Table 5	Supersaturation, time, and temperature of the nesquehonite to hydromagnesite transition.
Table 6	Parameters of heating schedule and the associated grain size results.

Sirine Guermech : Conceptualization, Methodology, Formal analysis, Investigation, Writing - Original Draft.

Julien Mocellin : Conceptualization, Methodology, Formal analysis, Investigation, Writing - Review & Editing, Supervision

Lan-Huong Tran : Conceptualization, Methodology, Formal analysis, Investigation, Writing - Review & Editing, Supervision.

Guy Mercier : Conceptualization, Methodology, Investigation, Writing - Review & Editing, Supervision, Funding acquisition.

Louis-César Pasquier : Project administration Conceptualization, Methodology, Investigation, Writing - Review & Editing, Supervision, Funding acquisition.

Highlights

- The grain size of magnesium carbonates depends on both temperature and supersaturation
- Impurities present in parent solution didn't interfere with the precipitation phase.
- Transition phenomenon from nesquehonite to hydromagnesite is affected by temperature only.
- The grain size distribution of the obtained minerals are larger than those issued from synthetic solutions in literature.

Declaration of interests

The authors declare that they have no known competing financial interests or personal relationships that could have appeared to influence the work reported in this paper.

The authors declare the following financial interests/personal relationships which may be considered as potential competing interests: